energy&fuels

Article

pubs.acs.org/EF

Mathematical Modeling of Coal Gasification Processes in a Well-Stirred Reactor: Effects of Devolatilization and Moisture Content

Jian Xu and Li Qiao*

School of Aeronautics and Astronautics, Purdue University, West Lafayette, Indiana 47907

ABSTRACT: The devolatilization process and the moisture content in coal and biomass play an important role on the gasification performance of these fuels. To theoretically understand the complex chemical processes in a gasifier, we developed a multiphysics model to simulate the gasification processes in a well-stirred reactor. This model is a first-of-its-kind: it considers detailed gas-phase chemistry, drying and devolatilization kinetics, particle-phase reactions, boundary layer diffusion, pore evolution, as well as full coupling between the two phases at various scales for mass, species, and energy exchange. Numerical simulations were conducted using an in-house code to understand the comprehensive gasification process, and the focus was on the effects of devolatilization and moisture content. Sensitivity analysis was performed to identify the most influential parameters among various chemical and physical processes on the overall gasification performance (conversion time and syngas production). The results show that the syngas yield is most sensitive to the reaction rates of carbon-steam and carbon-CO_2 reactions; the rates of drying and devolatilization have little impact on the syngas composition. The coal conversion time is most sensitive to the heat transfer rates including both radiation and convection, and its secondary sensitivity is to the reaction rate of the carbon-steam reaction. Lastly, the coal conversion time increases with increasing moisture content. This is because high moisture content causes a decrease of temperature, which reduces the reaction rates.

1. INTRODUCTION

Fuel synthesis through coal gasification can potentially provide a solution to the increasing demand of energy and liquid fuels for transportation. Understanding the complex chemical processes of coal gasification, both experimentally and computationally, has received increasing interest in recent years. In a previous work,[1] we developed a multiphysics model to simulate the gasification processes in a well-stirred reactor containing uniformly distributed carbon particles. This model considered detailed gas-phase and particle-phase reactions as well as full coupling between the two phases at various scales for mass, species, and energy exchange. The gas-phase reactions are described with detailed chemistry and variable thermodynamic and transport properties. The rates of heterogeneous surface reactions are simulated by the diffusion-kinetic model with consideration of boundary layer diffusion. Numerical simulations were conducted to understand the effects of pressure, O_2 concentration, and H_2 addition on the carbon gasification process. It is noted that this model considered gasification of carbon particles; it did not include drying and devolatilization processes that occur in the gasification process of real coal and biomass materials.

Devolatilization plays an important role in coal and biomass gasification. The gasification rate of various coals with different chemical composition is affected primarily through the devolatilization process. The devolatilization process also have a strong effect on char reactivity.[2,3] Therefore it is critical to include the devolatilization process when modeling coal gasification, especially the pyrolysis rate and volatile product composition. A number of kinetic models have been developed for the devolatilization of various coals. Models that are relatively simple include the single kinetic rate model[4] and the two competing rates model.[5] Complex models include the functional group-devolatilization vaporization cross-linking model,[6] the FLASHCHAIN model,[7−9] and the chemical percolation devolatilization.[10] These models are applicable over a wide range of coal types, but they are extremely complex and are difficult to use for practical applications.

The moisture content of a coal or biomass also has a significant influence on the drying process and will therefore affect the subsequent processes, e.g., devolatilization, volatile matter evolution, as well as gasification processes.[11] These various processes may take place simultaneously, and their interactions still need to be better understood.[12] Agarwal et al.[12] developed a model that described the coupled drying and devolatilization processes of Mississippi lignite coal in fluidized beds. Their results showed that this model was adequate for low rank coals with low tar yields. For coals with higher tar yields, however, a more accurate model that considers coupled heat and mass transfer was suggested to describe the drying and devolatilization processes. Yip et al.[13] developed a mathematical model for low-rank coal pyrolysis. This model included the primary and secondary coal pyrolysis reactions and the char gasification reaction with the in situ steam which resulted from both coal inherent moisture and pyrolytic water. The results showed that the char yields during pyrolysis decreased with the increase of coal inherent moisture content and the decreases of particle size because of the higher heating rate and the pore diffusion effect for the smaller particles. This model provides great insight into the effect of moisture content during the devolatilization process. However, to investigate the integrated impact of the moisture content during both the

Received: May 21, 2012
Revised: August 12, 2012
Published: August 13, 2012

dx.doi.org/10.1021/ef3008745 | *Energy Fuels* 2012, 26, 5759−5768

devolatilization process and the char gasification process, a model which considers the two processes is still needed.

Motivated by the above, we incorporated the submodels of moisture evaporation and devolatilization into the coal gasification model we have previously developed. The multiphysics model considered detailed gas-phase chemistry, drying and devolatilization kinetics, and porous structure evolution, as well as full coupling between the two phases, including species, mass, and energy exchange. The goal was to understand the complex gasification processes of coal in a well-stirred reactor, especially the effect of the moisture drying and the devolatilization process on the gasification performance under various conditions.

2. MODEL DESCRIPTION

A multiphysics model was developed to simulate the complex coal gasification processes in a well-stirred reactor. Major assumptions of the model include: the species inside the reactor are well-mixed; the pressure of the reactor remains constant; and the mass of the reactor is constant. The reason for choosing this model was because we wanted to focus on the effect of transient chemical kinetics (including coupled gas-phase kinetics and surface kinetics) by neglecting transport (assuming strong mixing) as well as fluid dynamics (e.g., reactants such as coal particles and steam are typically injected into a gasifier in practical applications).

Figure 1 shows a schematic of the well-stirred reactor. Although it is spherical, the reactor need not be of any particular geometric shape. Carbon particles with diameter d_p are uniformly distributed inside the reactor together with gaseous species. The reactor's pressure remains constant, which means that during the gasification process the volume increases as a result of thermal expansion; thus, the number density of coal particles N_p decreases but the total number is conserved. Under these assumptions, the gasification process inside the reactor is time-dependent and spatial-independent. Intense mixing is assumed so that all gas-phase properties are uniform or spatially independent, with the exception of the small boundary layers surrounding the particles. Within the boundary layer are mass, species, and energy exchanges between individual particles and the surrounding gases, causing local gradients. The model developed for a single particle, which includes multiple processes such as moisture drying, devolatilization, surface reactions, diffusion onto particle surface, and heat and mass transfer between the particle and the surrounding gases, statistically represents all particles inside the reactor. For the gas-phase reactions, detailed kinetics and variable thermodynamic and transport properties are considered. The governing equations of mass, species, and energy conservation for the two phases are coupled to account for exchange between the phases. The transient gasification process is computed until 99% (by total mass) of the coal particle is gasified.

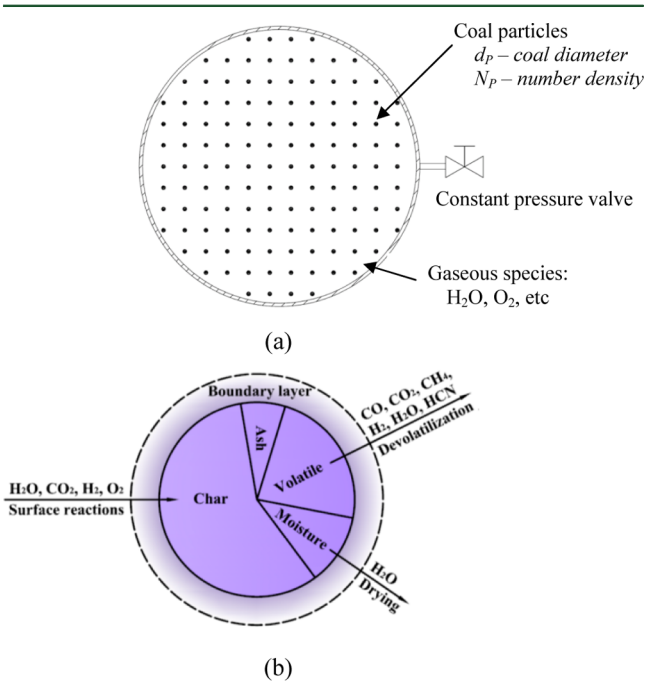

Figure 1. (a) Schematic of coal gasification in a constant-pressure well-stirred reactor and (b) schematic of multiple physical and chemical processes on a single coal particle.

2.1. Gas-Phase Equations. The conservation equations of mass, species, and energy for the gas phase are given as

$$\frac{dm_g}{dt} - \frac{m_g}{\rho_g}\sum w_i W_i = 0 \tag{1.1}$$

$$\rho_g \frac{dY_i}{dt} + Y_i \sum_{K=1}^{K} w_k W_k - (\omega_i + w_i)W_i = 0 \tag{1.2}$$

$$\rho_g \bar{C}_{p,g}\frac{dT_g}{dt} + \sum_i h_i(\omega_i + w_i)W_i - N_p(\dot{Q}_M + \dot{Q}_D + \dot{Q}_h + \dot{Q}_{conv,g}) = 0 \tag{1.3}$$

In eq 1.1, m_g and ρ_g are the mass and density of all gas-phase species, respectively; w_i is the molar production rate of species i because of drying, devolatilization, and surface reactions; W_i is the molecular weight of species i. In eq 1.2, Y_i is the mass fraction of species i; ω_i is the molar production rate of species i because of gas-phase reactions. In eq 1.3, $\bar{C}_{p,g}$ is the mean heat capacity of the gas mixture, which is determined by the detailed gas-phase kinetics; T_g is the gas-phase temperature; N_p is the particle-number density; h_i is the enthalpy of species i; $\dot{Q}_M$, $\dot{Q}_D$, and $\dot{Q}_h$ represent enthalpy transfer resulting from mass transfer because of drying, devolatilization, and surface reactions, respectively; and $\dot{Q}_{conv,g}$ is the convection heat transfer between a particle and its surrounding gases, which was calculated based on a Nusselt number of 2.[1]

A detailed gas-phase reaction mechanism, GRI-Mech 1.2, is incorporated into the model, which includes 177 elementary reactions and 32 species. The gas-phase species are H_2, H, O, O_2, OH, H_2O, HO_2, H_2O_2, C, CH, CH_2, $CH_2(S)$, CH_3, CH_4, CO, CO_2, HCO, CH_2O, CH_2OH, CH_3O, CH_3OH, C_2H, C_2H_2, C_2H_3, C_2H_4, C_2H_5, C_2H_6, HCCO, CH_2CO, HCCOH, and N_2. Variable thermodynamic and transport properties were adopted based on the CHEMKIN format. GRI-Mech 3.0 mechanism was also used, and the results are essentially the same as those of GRI-Mech 1.2.

2.2. Particle-Phase Equations. The particle mass m_p, diameter d_p, density ρ_p, number density N_p, and temperature T_p are the five variables to solve. The governing equations are

$$\frac{dm_p}{dt} = \frac{\sum w_i W_i}{N_p} = \dot{m}_M + \dot{m}_D + \dot{m}_C \tag{2.1}$$

dx.doi.org/10.1021/ef3008745 | Energy Fuels 2012, 26, 5759–5768

$$d_p = d_{p,0} \tag{2.2}$$

$$\rho_p = \rho_{p,0}\frac{m_p}{m_{p,0}} \tag{2.3}$$

$$N_p = N_{p,0}\frac{\rho_g}{m_g} \tag{2.4}$$

$$m_p C_{p,p}\frac{dT_p}{dt} = \dot{Q}_M + \dot{Q}_D + \dot{Q}_C + \dot{Q}_{conv,p} + \dot{Q}_{rad,p} \tag{2.5}$$

where, $\rho_{p,0}$, $m_{p,0}$, $d_{p,0}$, and $N_{p,0}$ are the initial density, mass, diameter, and number density of each particle at $t = 0$ s. The coal consumption rates are $\dot{m}_M$, $\dot{m}_D$, and $\dot{m}_C$ because of drying, devolatilization, and surface reactions, respectively; $C_{p,p}$ is the heat capacity of particles, which is calculated by JANAF Thermochemical Tables;[14] $\dot{Q}_{conv,p}$ is the convective heat transfer between a particle and the bulk gases, expressed as $\dot{Q}_{conv,p} = -\dot{Q}_{conv,g}$ (see eq 1.3); and $\dot{Q}_{rad,p}$ is the radiative heat transfer between a particle and the wall. Zedtwitz et al.[15] found that the radiation between the particles and the ambient dominates in the total radiative heat transfer in the reactor, which is 3 orders of magnitude higher than that the radiative heat transfer between the bulk gas and the ambient. As a result, other radiative heat transfer terms, e.g., between particles, between a particle and the bulk gases, and between the bulk gas and the wall, were neglected here.

The models, assumptions, and mechanisms for char gasification are similar to those in the previous study.[1] The difference is that the previous study considered carbon particles, whereas the present study considers a high-volatile coal. As a result, a moisture evaporation term and a devolatilization term were added to the mass and energy equation, respectively. The Carbon Burnout Kinetics (CBK), a kinetics package that describes char conversion developed by Sandia National Laboratories,[16] was used to describe the variation of particle diameter, density, number, and density during gasification. With this model, we assume a constant external diameter d_p (eq 2.2) and a linear relationship between particle density and mass (eq 2.3). Furthermore, the char surface area evolves during gasification and usually results in a porous structure. The Random Pore Model[17,18] has been widely used to quantitatively describe the evolution. The present work adapted the Random Pore Model by imposing a factor f_{RPM} into the gasification rate.[16] This factor accounts for the pore surface evolution because of carbon conversion:

$$f_{RPM} = \sqrt{1 - \psi_0 \ln(1 - x)} \tag{2.6}$$

where x is the carbon conversion ratio; ψ_0 is a structural parameter with an empirical value in a range of 2.2–7.7 [16] for most chars. Here a mean value of 4.6, as suggested in ref 16 was used.

2.3. Moisture-Drying Model. When coal particles are being heated up, the trapped moisture starts to evaporate, which is primarily a physical process but may also consist of chemical decomposition processes. Among the various methods of modeling, the moisture-drying process, the most common one, is to treat the drying process as an additional chemical reaction, and the reaction rate can be expressed in first-order Arrhenius form:[19,20]

$$\text{moisture} \xrightarrow{k_M} \text{water vapor} \tag{3.1}$$

The rate parameters are shown in Table 1.

Table 1. Reaction Rate Constants and Heat of Reaction

reaction	$K_k = B_k \exp(-E_k/T_p)$ B_k	E_k	$\dot{Q}$ (10^7 erg/g)
moisture drying[20]	5.13×10^{10}	8.8×10^4	2 440
devolatilization[26]	1×10^5	12 000	979.52
surface reaction A[32,33]	247	21 060	9 908
surface reaction B[32,33]	247	21 060	13 310
surface reaction C[33,34]	0.12	17 921	−7 283
surface reaction D[33,34]	8 710	17 967	$-2(1 - 1/\phi) \times 10\,260 - (2/\phi - 1) \times 33\,830$

2.4. Devolatilization Model. Eleanor Binner et al. [21] experimentally studied the effect of coal predrying on the concentrations of inorganic species present in the coal combustion. The results showed that the pyrolysis rate is similar for both dry and wet coals. Therefore, the same devolatilization kinetics can be used for both predried coal and wet coal. The devolatilization process of a coal is indeed complicated. The volatile yield and composition are influenced by several factors, especially coal type.[22] In the present study, we choose Illinois No. 6 coal: its proximate and ultimate analyses are listed in Table 2. Following Bradley et al.,[23] a one-step global devolatilization model was used to estimate the pyrolysis rate, which has a first-order Arrhenius expression, as shown in Table 1. In the following, we will discuss the volatile composition.

Table 2. Proximate and Elemental Analyses of Illinois No. 6 Coal

proximate analysis	as received, wt %	dry, wt %	ultimate analysis	dry ash-free (daf), wt %	daf without sulfur, wt %
moisture	3.2		C	77.2	80.25
fixed carbon	52.0	53.8	H	5.2	5.40
volatile matter	35.0	36.1	O	12.3	12.79
ash	9.8	10.1	N	1.5	1.56
			S	3.8	

For Illinois No. 6 coal, devolatilization is a two-step process: the first step yields tar, primary gaseous volatiles (CH_4, HCN, H_2, CO, CO_2, and H_2O), and residual char; in the second step, the tar yields secondary gaseous volatiles (CH_4, HCN, H_2, and CO) and residual soot. To calculate the mass fractions of the eight volatile species in the first step, we followed the method of Merrick.[24] To be specific, five species are based on mass conversation of the ultimate (C, H, O, and N) and proximate (char) analyses of the coal shown in Table 2; the remaining three are listed as eqs 4.1–4.3, which are based on the findings of Xu and Tomita[25] that the dry-ash-free mass fraction of CO and H_2O varied linearly with the mass fraction of O and there is a reasonable correlation between the dry-ash-free mass fractions of tar and the proximate volatile matter $[VM]_f$. These relations were found for 17 different coals, ranging from lignite to anthracite and including the coal studied in the present work.

dx.doi.org/10.1021/ef3008745 | Energy Fuels 2012, 26, 5759–5768

$$\frac{16}{28}[\mathrm{CO}]_f = 0.1657 m_{fO} \quad (4.1)$$

$$\frac{16}{18}[\mathrm{H_2O}]_f = 0.2933 m_{fO} \quad (4.2)$$

$$[\mathrm{tar}]_f = 0.48\,[\mathrm{VM}]_f \quad (4.3)$$

The product composition for tar secondary devolatilization (soot, CH_4, HCN, H_2, and CO) was obtained using four equations based on the elemental composition of the tar and a fifth equation based on an assumption of equality of the ratios of H_2 to CH_4 in the primary and secondary volatiles. Solution of the above-mentioned equations yields the mass fractions of the six gaseous volatiles, the char, the ash, and the soot: 4.0% CH_4, 0.4% HCN, 3.4% H_2, 7.2% CO, 5.5% CO_2, 3.8% H_2O, 53.8% char, 10.1% ash, and 11.8% soot.

In the present model, HCN was neglected because of its relative small content. Soot was assumed to be predominantly carbon, and ash was assumed to remain on the char during gasification.

2.5. Char Surface Reactions. Four heterogeneous reactions are assumed to take place on the particle surfaces:

$$\mathrm{C + H_2O \rightarrow CO + H_2} \quad (A)$$

$$\mathrm{C + CO_2 \rightarrow 2CO} \quad (B)$$

$$\mathrm{C + 2H_2 \rightarrow CH_4} \quad (C)$$

$$\mathrm{C + 1/\phi O_2 \rightarrow 2(1 - 1/\phi)CO + (2/\phi - 1)CO_2} \quad (D)$$

Reaction D is the char-oxygen reaction, which can produce both CO and CO_2. The ratio of CO to CO_2 depends on particle size and temperature. The empirical parameter ϕ in reaction D is obtained as follows.[26]

$$\phi = \begin{cases} (2Z + 2)/(Z + 2) & \text{for } d_p \le 0.005 \text{ cm} \\ [(2Z + 2) - Z(d_p - 0.005)/0.095] & \\ \quad /(Z + 2) & \text{for } 0.005 \text{ cm} \\ \quad < d_p & \\ \quad \le 0.1 \text{ cm} & \\ 1.0 & \text{for } d_p > 0.1 \text{ cm} \end{cases} \quad (5.1)$$

$$Z = 2500 \exp(-6249/T) \quad (5.2)$$

$$T = (T_p + T_g)/2 \quad (5.3)$$

The global rate of each reaction was simulated using the diffusion-kinetic model,[27] which is of the first order for reactions A, B, and D and of the second order for reaction C. The carbon reaction rate can be written as

$$\dot{m}_{C,k} = -A_p K_k (P X_{k,s})^n \quad (5.4)$$

where subscription k denotes reactions A, B, C, or D; K_k is the surface reaction rate constant; $X_{k,s}$ is the mole fraction of the gaseous reactant at the particle surface. The surface reaction rate constant is expressed in Arrhenius form as

$$K_k = B_k \exp\left(-\frac{E_k}{RT_p}\right) \quad (5.5)$$

where B_k is the prefactor, and E_k is the activation energy. The kinetic constant and the references from which they were obtained are listed in Table 1.

The transport rate of reactant gases to carbon surface was determined by bulk diffusion through an external boundary layer as discussed in the previous study.[1] The mole fractions of the reactant gases (H_2O, CO_2, H_2, and O_2) at the particle surface ($X_{k,s}$) and in the bulk ($X_{k,\infty}$) are correlated by a closed nonlinear system of transport equations in the boundary layer that surrounds the particle. Given the mole fraction of the gases in the bulk, the system can be solved to obtain their mole fraction at the particle surface. Pore diffusion through an ash layer that could form over the char surface during later stages of gasification was neglected. The impact of the internal porous structure on the surface reaction rate was accounted for by the random pore model, as discussed in the previous section.

3. RESULTS AND DISCUSSIONS

Numerical simulations were conducted to gain a fundamental understanding of the coal gasification processes. Sensitivity analyses were performed to identify the most influential parameters for gasification performance. Illinois No. 6 coal was used in this study, which consists of 3.2% moisture and 35.0% volatile matter, as shown in Table 2. Partial oxidation of coal was considered to provide the heat needed for the endothermic gasification reactions. The coal particles were fed into the reactor at room temperature; the mixture of steam and oxygen was preheated up to 1120 K. The reactor wall temperature was assumed to be constant at 500 K. The initial H_2O/C ratio was 2, and the particle size was 100 μm. All parameters used in the present simulation are listed in Table 3. In the following we will discuss the general characteristics of the gasification process.

Table 3. Initial Conditions for Gasification of Illinois No. 6 Coal

initial gas temperature	T_g = 1120 K	initial particle temperature	T_p = 300 K
wall temperature	T_W = 500 K	density of particles	ρ_p = 1.3 g/cm^3
gas pressure	P = 10 atm	initial particle diameter	d_p = 100 μm
initial steam concentration	X_{H_2O} = 0.85	initial oxygen concentration	X_{O_2} = 0.15
initial H_2O/coal molar ratio	H_2O/coal = 2.0	particle number density	Np = 911/cm^3

3.1. Temperature and Species Concentration Profiles. Figure 2a shows the molar fraction profiles of five stable species (H_2, H_2O, O_2, CO, and CO_2) as well as the coal conversion rate as functions of time. Figure 2b shows the molar fractions of four minor species (H, OH, CO_4, and CH_2O) as well as the particle (T_p) and gas temperatures (T_g) as functions of time. Between 0 and 0.1 s, T_g decreases slightly, mainly because the moisture evaporation process and the devolatilization process both absorb heat. During this time, however, particles are being heated up from 300 K; their temperature continues to increase to about 1000 K, which is high enough for volatile to be released from the particles. At around 0.075 s, we observe that the molar fractions of H_2, CO, and CH_4 reach a peak as a result of devolatilization. At around 0.10 s, both T_p and T_g start to rise quickly. At the same time, the molar fraction of O_2 drops to zero and a peak exists for the molar fraction of OH radical,

dx.doi.org/10.1021/ef3008745 | Energy Fuels 2012, 26, 5759−5768

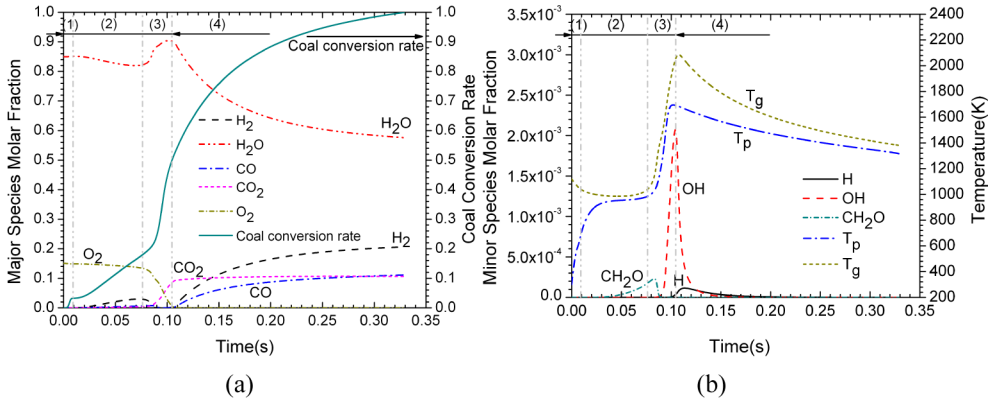

Figure 2. Profiles of the species molar fraction, coal conversion time, and particle and gas temperatures as functions of time. (a) Major species molar fraction and coal conversion time and (b) minor species molar fraction and particle and gas temperatures.

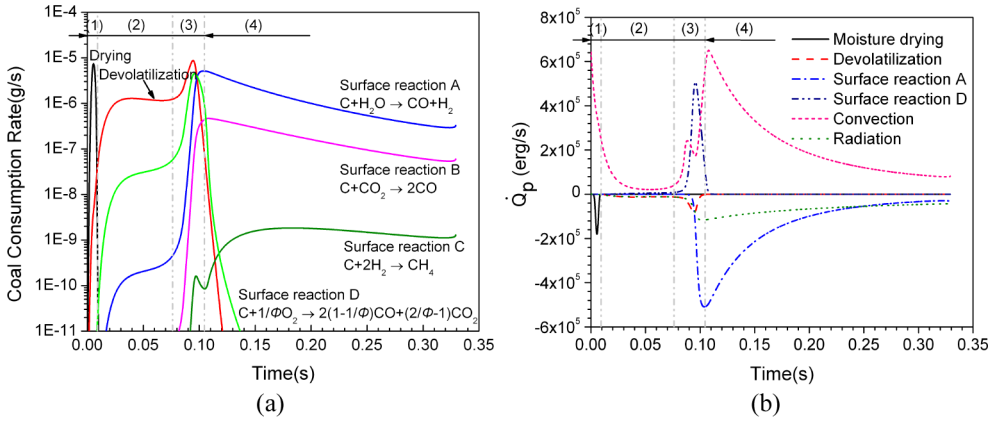

Figure 3. Profiles of coal consumption rate and heat release rate based on a single particle: (a) coal consumption rate because of drying, devolatilization, and surface reactions and (b) heat absorption/release because of drying, devolatilization, surface reactions, convection, and radiation.

indicating the occurrence of the combustion of volatile species in the gas phase. This also indicates that the ignition process is initiated by the ignition of the volatile, which is consistent with the experimental results of Molina et al.[28] and McLean et al.[29] After the volatile combustion is completed, the molar fractions of H_2 and CO start to increase and the particle and gas temperatures to decrease, all because of the endothermic gasification reactions. The gasification process takes about 0.33 s, and the final products include 20.6% H_2, 57.6% H_2O, 11.1% CO, and 10.6% CO_2.

Figure 2b shows T_g decreases to 990 K, from 1120 K, during 0−0.05 s, and they then increase quickly to the peak 2090 K. Two sharp increases are experienced by T_p, to 950 K, from 300 K, during 0−0.05 s, and to 1700 K, from 950 K, during 0.05−0.10 s. The changes of T_p are the result of the complex gasification processes, which include moisture drying, devolatilization, surface reactions, and convective heat transfer between the particle and the gas bulk, and the radiation between the particle and the wall. In the following we discuss the relative importance of these processes.

3.2. Particle-Phase Reaction Rates and Energy Transfer. Figure 3a plots the mass reduction rate of each coal particle because of drying, devolatilization, and surface reactions. The results show that the drying process is most dominant at the beginning, which lasts for about 0.01 s. From 0.01 s to 0.10 s, devolatilization is the dominant process. After 0.10 s, the surface reactions A, B, and C have the greatest coal consumption rates. Especially, the rate of the C + H_2O → CO + H_2 reaction is almost 10 times and 1000 times faster than the rates of the C + CO_2 → 2 CO and C + 2 H_2 → CH_4 reactions, respectively. Noticeably, around t = 0.1 s, the carbon oxidation reaction C + O_2 → CO + CO_2 has a peak rate for a relatively short time. This indicates that the gas-phase and particle-phase oxidation reactions were taking place nearly simultaneously, both competing for O_2 in the gas phase.

Figure 3b plots the heat absorption or release of the above-mentioned processes, all based on one single particle. Because the particles were entering the reactor at room temperature and the gas mixture (H_2O/O_2) was at 1120 K when entering the reactor, there was a strong convective heat transfer between the two phases. This energy transfer provides the heat needed for moisture drying and devolatilization during 0−0.09 s as shown in Figure 3b. Around 0.10 s, the heat release from char oxidation produces the most energy (heat release) for the particle. After 0.10 s, when oxygen had been completed and the gas temperature had increased significantly because of the volatile combustion, the convection heat transfer dominates again in providing the heat needed for the endothermic gasification reactions.

In summary, we can divide the gasification process into four stages: (1) drying, (2) devolatilization, (3) volatile combustion and char combustion, and (4) char gasification, as shown in Figures 2 and 3. Although the drying, devolatilization, char combustion, and gasification processes overlap with one another, the four stages can be easily determined by the most significant one. During drying and devolatilization, steam from

dx.doi.org/10.1021/ef3008745 | Energy Fuels 2012, 26, 5759−5768

moisture evaporation and volatiles from pyrolysis diffuse outwardly.

Because of their endothermic nature, heat must be provided. Volatile combustion and the char combustion process feature the rapid increase of temperatures. In the gas-phase, H_2 and CO are depleted by the oxidation with O_2. In the meantime, the char-O_2 surface reaction also competes for O_2. In Figure 3b, the convection rate starts to increase in stage 3 at 0.08 s, while the surface reaction D ($C + O_2 \rightarrow CO + CO_2$) at 0.09 s, indicating the volatile combustion, is slightly ahead of the char combustion and provides the energy to trigger its reaction. After the release of moisture and volatile is completed, the char gasification process becomes dominant in coal consumption and heat absorption, especially the reaction $C + H_2O \rightarrow CO + H_2$.

3.3. Gas-Phase Reaction Rates. From Figure 2b, we can see that the volatile combustion occurs around 0.10 s. To determine the most important gas-phase reactions during the process, we examined the 177 detailed elementary reactions and identified 7 that have the highest mole production rate, as shown in Figure 4. These reactions are $H + O_2 + H_2O_2 \Leftrightarrow HO_2 + H_2O$, $OH + H_2 \Leftrightarrow H + H_2O$, $2HO_2 \Leftrightarrow O_2 + H_2O_2$, $OH + CO \Leftrightarrow H + CO_2$, $OH + HO_2 \Leftrightarrow O_2 + H_2O$, $2OH\ (+ M) \Leftrightarrow H_2O_2\ (+ M)$, and $2OH \Leftrightarrow O + H_2O$. These reactions indicate that the volatile combustion mechanism mainly consists of the oxidation of H_2 and CO. Moreover, the oxidation rate of H_2 (mainly by $H + O_2 + H_2O \Leftrightarrow HO_2 + H_2O$ and $OH + H_2 \Leftrightarrow H + H_2O$) is much faster than that of CO (mainly by $OH + CO \Leftrightarrow H + CO_2$).

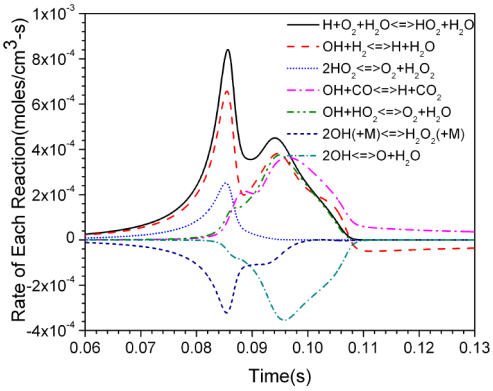

Figure 4. Reaction rate of the main gas-phase elementary reactions as a function of time.

3.4. Boundary Layer Diffusion. In the present study, four surface reactions (char − H_2O, char − CO_2, char − H_2, and char − O_2) were assumed to take place on the particle surface and in the pore. Their overall reaction rates depend on the reaction rate constants as well as on the diffusion rate of the reactant gases (H_2O, CO_2, H_2, and O_2) onto the particle surface within the boundary layer. During the devolatilization process, volatile species diffuse out from the particle surface to the bulk gases and then participate in gas-phase reactions. The bulk gaseous reactants such as H_2O diffuse onto the particle surface, resulting in a surface reaction. The multicomponent diffusion process interacts with other processes such as devolatilization, volatile combustion, and surface reactions, causing a dynamic change of these species in the bulk and within the boundary layer.

Figure 5 shows the ratio of the mole fraction of several species (including CO_2, H_2O, H_2, and O_2) at the particle surface to the mole fraction in the gas bulk as a function of time ($X_{k,s}/X_{k,\infty}$). Before 0.10 s, the molar fractions of CO_2 and H_2 are much higher at the particle surface than in the gas bulk. This is because the volatiles are being released continuously. At around 0.10 s, the molar fraction of H_2 in the gas bulk drops quickly, which leads to a large molar fraction ratio at particle surface and in the bulk. This is due to volatile combustion (oxidation of H_2 and CO, as shown in Figure 4), which consumes H_2 and CO. From 0.15 s to the end of the gasification process, during which time the surface reactions dominate as shown in Figure 3, the diffusion of H_2O, CO_2, and H_2 is very fast: these species reach equilibrium at the particle surface and in the gas bulk.

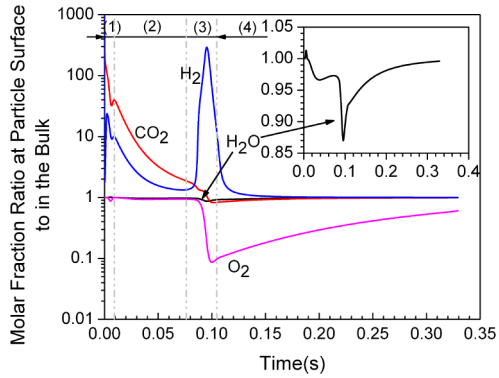

Figure 5. Ratio of the molar fraction of the main species at the particle surface to the molar fraction in the gas bulk as a function of time.

3.5. Sensitivity Analyses. Coal gasification is a complex phenomenon involving multiple chemical and physical processes: drying, devolatilization, volatile combustion, char oxidation, char gasification, convective and radiative heat transfer, and boundary layer diffusion. A submodel for each of these processes will be needed to simulate the complex gasification process in real gasifiers. The submodels, however, may not be accurate or have not been widely validated. So the question is this: how is the gasification performance sensitive to these submodels, especially the rate parameters such as devolatilization rate, drying rate, gas-phase reaction rates, surface reaction rates, and heat transfer coefficient?

Motivated by the above, we conducted a sensitivity analysis for the case discussed previously (the initial conditions are summarized in Table 3). The sensitivity coefficient is defined as

$$A_i = \frac{R_i}{y}\frac{\Delta y}{\Delta R_i}$$

where A_i is the sensitivity coefficient, y is the examined parameters, gasification performance including the molar fractions of H_2 and CO in the syngas and the coal conversion time, and R_i is the model parameters including the drying rate, devolatilization rate, surface reaction rates of reactions A−D, as well as the convective and radiation heat transfer coefficients. The sensitivity coefficient was obtained based on the "brute-force" method that one of the model parameters was artificially perturbed by 10% while keeping all other parameters fixed.

Figure 6a shows the sensitivity coefficients with respect to the above-mentioned reaction/heat transfer rates. Among the model parameters, the rates of surface reaction A ($C + H_2O \rightarrow$

dx.doi.org/10.1021/ef3008745 | Energy Fuels 2012, 26, 5759−5768

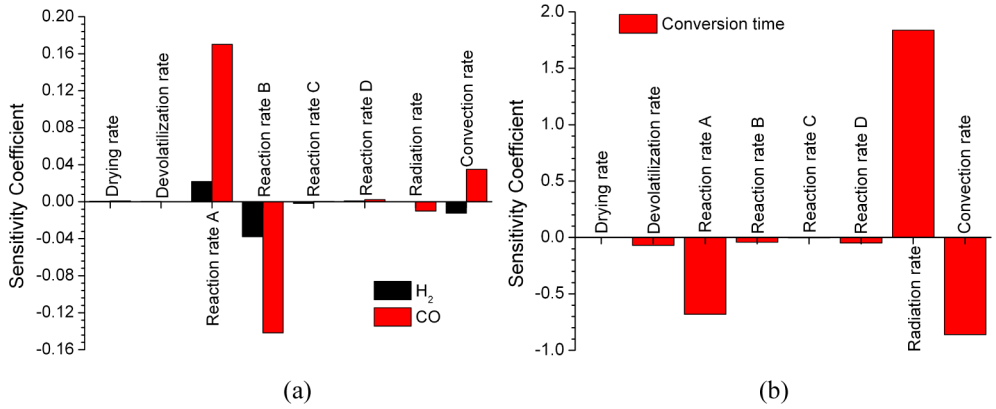

Figure 6. Sensitivity coefficients with respect to the reaction rate and reaction heat: (a) sensitivity coefficient of the H_2 and CO molar fractions and (b) sensitivity coefficient of the coal conversion time.

CO + H_2) and B (C + CO_2 → 2 CO) have the most influence on the final syngas composition, whereas the drying rate and the devolatilization rate as well as the rates of surface reactions C and D all have little effect on the final molar fractions of H_2 and CO. Surface reaction A is dominant during the char-gasification process. Therefore the increase of the rate of surface reaction A will promote the char-steam reaction and produce more H_2 and CO. The increase of the rate of surface reaction B, on the contrary, will weaken the dominance of surface reaction A (char − H_2O). This will lead to less H_2 and CO generated by reaction A and more H_2O left in the final gas composition. The increase of H_2O greatly decreases the molar fractions of H_2 and CO in the final product. The rates of drying and devolatilization have little impact on the syngas yield. This is because H_2 and CO produced from the devolatilization process have been completely burned during the volatile combustion process. Therefore the syngas yield is mainly dependent on the char gasification process that follows the volatile combustion process.

Figure 6b shows the sensitivity coefficients of the coal conversion time with respect to the reaction/heat transfer rates. The coal conversion time is the most sensitive to the radiative heat transfer rate, convection heat transfer coefficient, and the rate of reaction A. As for the drying rate, the devolatilization rate, and the rates of surface reactions B, C, and D have much a smaller effect on the coal conversion time. In summary, the convective heat transfer between the two phases and the radiative heat transfer (emission and absorption) within particles have a controlling effect on particle temperature, which determines the reaction rate and thus the overall conversion time.

3.6. Effect of Moisture. The moisture content of the coal has a great impact on the overall gasification process.[11,30] The drying process increases the H_2O concentration at the particle surface and in the pore, which may promote the char-steam surface reaction. On the other hand, the heat absorbed by moisture evaporation will decrease the particle and gas temperatures, which leads to lower rates of devolatilization and surface reactions. To understand these competing effects of moisture on the overall gasification performance, we artificially varied the moisture content in the Illinois No. 6 coal: it was increased to 12% from 0%. The total mass of the fixed carbon, volatile matter, and ash, however, remained unchanged (their composition based on dry-basis is shown in Table 2). The particle densities corresponding to various moisture content are 1.258 g/cm^3 for 0% moisture content, 1.3 g/cm^3 for 3.2% moisture content, 1.339 g/cm^3 for 6% moisture content, 1.368 g/cm^3 for 8% moisture content, 1.398 g/cm^3 for 10% moisture content, and 1.43 g/cm^3 for 12% moisture content. All other initial conditions are the same as shown in Table 3.

To better understand how the gasification process is affected by the moisture content, we first plotted the profiles of the particle and gas temperatures as functions of time at 3.2%, 8%, and 12% moisture content, as shown in Figure 7. Higher

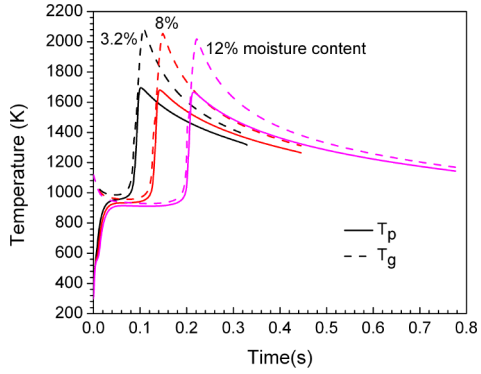

Figure 7. Profiles of the particle and gas temperatures as functions of time at moisture content of 3.2%, 8%, and 12%.

moisture content leads to lower gas and particle temperatures throughout the entire process. Both the drying and devolatilization process lasted longer because of the lower temperatures. The volatile combustion and char oxidation process were therefore delayed. During the char gasification process (the mass of char was kept constant), the lower temperatures led to lower surface reaction rates and thus longer conversion time.

Figure 8 shows a comparison of the mass reduction rates and heat absorption or release rates of one particle because of drying, devolatilization, and surface reactions at a moisture content of 3.2% and 12%, respectively. The results show that both drying processes at a moisture content of 3.2% and 12% are orders of magnitude shorter than those of char gasification. Therefore this process can be assumed to take place instantaneously, as many studies in the literature did.[31] Because of the lower temperatures caused by the higher moisture content, the coal consumption rates at 12% moisture content resulting from devolatilization and surface reactions are lower

dx.doi.org/10.1021/ef3008745 | Energy Fuels 2012, 26, 5759−5768

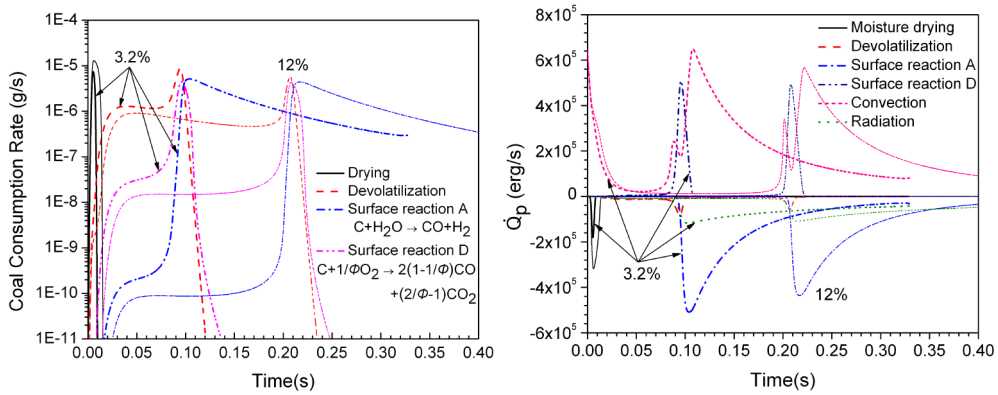

Figure 8. Profiles of coal consumption rate and heat release based on a single particle at moisture contents of 3.2% and 12%: (a) coal consumption rate because of drying, devolatilization, and surface reactions and (b) heat absorption/release resulting from drying, devolatilization, and surface reactions, convection, and radiation.

than those at 3.2% moisture content. Meanwhile, heat absorption/release rates because of devolatilization and surface reactions at 12% moisture content are also lower compared to those at 3.2% moisture content. These indicate that the effect of moisture mainly serves to inhibit the overall gasification rate as a result of the temperature drop. Also the impact of the moisture to impact char-steam reaction is negligible.

The effect of moisture content on the gasification performance, including the coal conversion time, the final syngas production, and the upgrade factor U, is shown in Figure 9 for three different particle sizes. The upgrade factor is defined as

$$U = \frac{m_{\text{syngas}}\text{LHV}_{\text{syngas}}}{m_{\text{feedstock}}\text{LHV}_{\text{feedstock}}}$$

where $m_{\text{feedstock}}$ and m_{syngas} are the mass of the gasified feedstock and the syngas, respectively; LHV is the lower heating value based on the individual components at 298 K.

The coal conversion time increases with the increase of the moisture content. However, the molar fractions of H_2 and CO in the dry gas mixture remain almost constant at various particle sizes (0.49 H_2 and 0.26 CO at 100 μm, 0.485 H_2 and 0.27 CO at 75 μm, and 0.48 H_2 and 0.28 CO at 50 μm). As discussed above, H_2 and CO were first depleted as a result of volatile combustion; they were regenerated during the char gasification process. At the beginning of char gasification, there was no difference between the particles with various moisture contents because all the moisture and volatile matter had been released prior to that. The gasification of the same amount of char thus produced almost constant molar fractions of H_2 and CO in a dry gas mixture. It also can be seen in Figure 9c that higher moisture content will lead to a lower upgrade factor (from 1.12 to 0.95 at 100 μm, from 1.16 to 1.05 at 75 μm, and from 1.20 to 1.08 at 50 μm). Because the final molar fractions of H_2 and CO remain almost constant, the upgrade factor is mainly determined by the amount of the consumed coal in a unit volume. At higher moisture content, the final particle number density is higher because of the lower final temperatures as shown in Figure 7. The higher number density will lead to higher coal consumption in a unit volume which will result in a lower upgrade factor. The effect of particle size can also be examined in Figure 9. With smaller particle size, the conversion time will be lower and the upgrade factor will be higher. As for the syngas production, decreasing particle size will increase the molar faction of CO while decreasing the molar faction of H_2.

4. CONCLUSIONS

To theoretically understand the complex chemical processes in a gasifier, especially the effects of the devolatilization process and the moisture content in coal/biomass, we developed a multiphysics model to simulate the gasification processes in a well-stirred reactor. This model is a first-of-its-kind: it considers detailed gas-phase chemistry, drying, and devolatilization kinetics, particle-phase reactions, boundary layer diffusion, and pore evolution, as well as full coupling between the two phases at various scales for mass, species, and energy exchange. The present numerical simulations lead to the following major conclusions: (i) In the coal gasification process with partial oxidation, the chemical processes in the reactor can be divided into four stages: (1) drying, (2) devolatilization, (3) volatile combustion and char oxidation, and (4) char gasification. In the first two stages, steam is evaporated from moisture drying, and volatiles are released during devolatilization. These two processes consume heat and cause the gas temperature to decrease. During the gas-phase volatile combustion and char oxidation process, because of the oxidation of H_2 and CO as well as char, the temperatures increase rapidly and this provides the energy needed in the followed char gasification process. Among the surface reactions, the carbon-steam reaction C + $H_2O \rightarrow$ CO + H_2 dominates in the char gasification process. (ii) Sensitivity analysis was performed to identify the most influential parameters among various chemical and physical processes on the overall gasification performance (conversion time and syngas production). The results show that the syngas yield is most sensitive to the reaction rates of char-steam and char-CO_2 reactions; the rates of drying and devolatilization have little effect on the syngas composition. The coal conversion time is most sensitive to the heat transfer rates, including both radiation and convection, and is secondary-sensitive to the reaction rate of carbon-steam reaction. (iii) The increase of the moisture content will increase the coal conversion time and decrease the upgrade factor. However, the molar fractions of H_2 and CO in a dry gas mixture remain almost constant. The effect of moisture mainly serves to inhibit the overall gasification rate because of the temperature drop. Its impact on the carbon-steam reaction is negligible. (iv) Decreasing the particle size will decrease the conversion time

dx.doi.org/10.1021/ef3008745 | Energy Fuels 2012, 26, 5759−5768

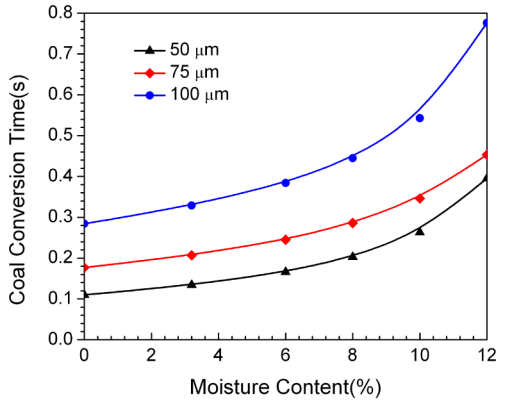

(a)

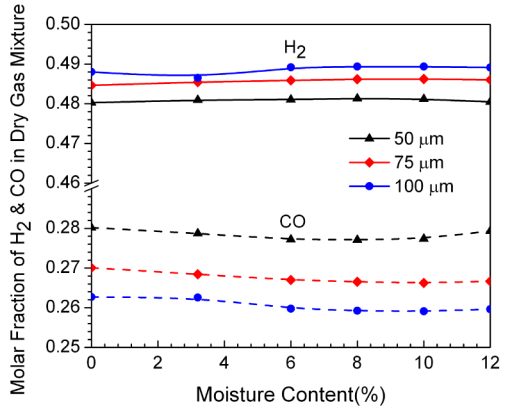

(b)

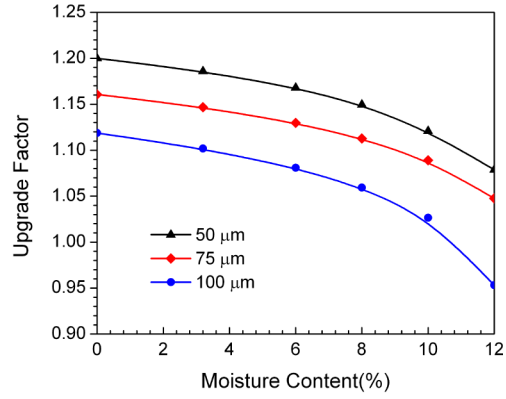

(c)

Figure 9. Profiles of the coal conversion time (a), the molar fraction of H_2 and CO in dry gas mixture (b), and the upgrade factor (c) as functions of the moisture content at three different particle sizes.

and increase the upgrade factor. As for the syngas production, decreasing the particle size will increase the molar faction of CO while decreasing the molar faction of H_2.

AUTHOR INFORMATION

Corresponding Author

*E-mail: lqiao@purdue.edu.

Notes

The authors declare no competing financial interest.

ACKNOWLEDGMENTS

This work was supported by the Air Force Office of Scientific Research under the technical management of Dr. Julian Tishkoff. Support for Jian Xu from the Purdue Energy Fund is also acknowledged.

REFERENCES

(1) Qiao, L.; Xu, J.; Sane, A.; Gore, J. Multiphysics modeling of carbon gasification processes in a well-stirred reactor with detailed gas-phase chemistry. *Combust. Flame* **2012**, *159* (4), 1693−1707.

(2) Anthony, D. B.; Howard, J. B. Coal Devolatilization and Hydrogasification. *AIChE J.* **1976**, *22* (4), 625−656.

(3) Khan, M. R.; Hshieh, F. Y., Influence of Steam on Coal Devolatilization and on the Reactivity of the Resulting Char. *Abstr. Pap. Am. Chem. Soc.* **1989**, *198*, 76-Fuel.

(4) Badzioch, S.; Hawksley, P. G. Kinetics of Thermal Decomposition of Pulverized Coal Particles. *Ind. Eng. Chem. Process Des. Dev.* **1970**, *9* (4), 521.

(5) Kobayashi, H.; Howard, J. B.; Sarofim, A. F. Coal devolatilization at high temperatures. In *18th Symposium (International) on Combustion*; The Combustion Institute: Pittsburgh, PA, 1977; Vol. *16*, pp 411−425

(6) Solomon, P. R.; Hamblen, D. G.; Carangelo, R. M.; Serio, M. A.; Deshpande, G. V. General-Model of Coal Devolatilization. *Energy Fuels* **1988**, *2* (4), 405−422.

(7) Niksa, S.; Kerstein, A. R. Flashchain Theory for Rapid Coal Devolatilization Kinetics 0.1. Formulation. *Energy Fuels* **1991**, *5* (5), 647−665.

(8) Niksa, S. Flashchain Theory for Rapid Coal Devolatilization Kinetics 0.2. Impact of Operating-Conditions. *Energy Fuels* **1991**, *5* (5), 665−673.

(9) Niksa, S. Flashchain Theory for Rapid Coal Devolatilization Kinetics 0.3. Modeling the Behavior of Various Coals. *Energy Fuels* **1991**, *5* (5), 673−683.

(10) Grant, D. M.; Pugmire, R. J.; Fletcher, T. H.; Kerstein, A. R. Chemical-Model of Coal Devolatilization Using Percolation Lattice Statistics. *Energy Fuels* **1989**, *3* (2), 175−186.

(11) Erdol, N.; Calli, L.; Okutan, H.; Arisoy, A.; Ekinci, E. Effect of coal moisture on particulate emission in a fixed bed combustion appliance. *Fuel Process. Technol.* **1999**, *58* (2−3), 109−117.

(12) Agarwal, P. K.; Genetti, W. E.; Lee, Y. Y., Drying and Devolatilization of Mississippi Lignite in a Fluidized-Bed. *Abstr. Pap. Am. Chem. Soc.* **1984**, *187*, (April), 28-Fuel.

(13) Yip, K.; Wu, H. W.; Zhang, D. K. Mathematical modelling of Collie coal pyrolysis considering the effect of steam produced in situ from coal inherent moisture and pyrolytic water. *Proc. Combust. Inst.* **2009**, *32*, 2675−2683.

(14) Trinh, C. M. *Numerical Modelling of One-Dimensional Laminar Pulverised Coal Combustion*; Laboratory of Heating and Air Conditioning, Technical University of Denmark: Kongens Lyngby, 1995.

(15) von Zedtwitz, P.; Lipinski, W.; Steinfeld, A. Numerical and experimental study of gas-particle radiative heat exchange in a fluidized-bed reactor for steam-gasification of coal. *Chem. Eng. Sci.* **2007**, *62* (1−2), 599−607.

(16) Liu, G. S.; Niksa, S. Coal conversion submodels for design applications at elevated pressures. Part II. Char gasification. *Prog. Energy Combust. Sci.* **2004**, *30* (6), 679−717.

(17) Bhatia, S. K.; Perlmutter, D. D. A Random Pore Model for Fluid-Solid Reactions 0.1. Isothermal, Kinetic Control. *AIChE J.* **1980**, *26* (3), 379−386.

(18) Bhatia, S. K.; Perlmutter, D. D. A Random Pore Model for Fluid-Solid Reactions 0.2. Diffusion and Transport Effects. *AIChE J.* **1981**, *27* (2), 247−254.

(19) Shi, S. P.; Zitney, S. E.; Shahnam, M.; Syamlal, M.; Rogers, W. A. Modelling coal gasification with CFD and discrete phase method. *J. Energy Inst.* **2006**, *79* (4), 217−221.

(20) Bryden, K. M.; Ragland, K. W.; Rutland, C. J. Modeling thermally thick pyrolysis of wood. *Biomass Bioenergy* **2002**, *22* (1), 41−53.
(21) Binner, E.; Facun, J.; Chen, L. G.; Ninomiya, Y.; Li, C. Z.; Bhattacharya, S. Effect of Coal Drying on the Behavior of Inorganic Species during Victorian Brown Coal Pyrolysis and Combustion. *Energy Fuels* **2011**, *25* (7), 2764−2771.
(22) Carpenter, A. M.; Skorupska, N. M. *Coal Combustion-Analysis and Testing*; IEACR/64; IEA Coal Research: London, 1993.
(23) Bradley, D.; Lawes, M.; Park, H. Y.; Usta, N. Modeling of laminar pulverized coal flames with speciated devolatilization and comparisons with experiments. *Combust. Flame* **2006**, *144* (1−2), 190−204.
(24) A Merrick, D. Mathematical-Models of the Thermal-Decomposition of Coal 1. The Evolution of Volatile Matter. *Fuel* **1983**, *62* (5), 534−539.
(25) Xu, W.-C.; Tomita, A. Effect of temperature on the flash pyrolysis of various coals. *Fuel* **1987**, *66* (5), 632−636.
(26) Govind, R.; Shah, J. Modeling and Simulation of an Entrained Flow Coal Gasifier. *AIChE J.* **1984**, *30* (1), 79−92.
(27) Zhou, L. X., *Theory and Numerical Modeling of Turbulent Gas-particle Flows and Combustion*; CRC Press: Boca Raton, FL, 1993.
(28) Molina, A.; Shaddix, C. R. Ignition and devolatilization of pulverized bituminous coal particles during oxygen/carbon dioxide coal combustion. *Proc. Combust. Inst.* **2007**, *31* (2), 1905−1912.
(29) McLean, W. J.; Hardesty, D. R.; Pohl, J. H. Direct observations of devolatilizing pulverized coal particles in a combustion environment. *Symp. (Int.) Combust.* **1981**, *18* (1), 1239−1248.
(30) Hughes, W. E. M.; Larson, E. D. Effect of fuel moisture content on biomass-IGCC performance. *J. Eng. Gas Turbines Power* **1998**, *120* (3), 455−459.
(31) Di Blasi, C. Dynamic behaviour of stratified downdraft gasifiers. *Chem. Eng. Sci.* **2000**, *55* (15), 2931−2944.
(32) Dobner, S. Modelling of Entrained Bed Gasification: The Issues. EPRI, Palo Alto, CA, January 15, 1976.
(33) Wen, C. Y.; Chaung, T. Z. Entrainment Coal-Gasification Modeling. *Ind. Eng. Chem. Process Des. Dev.* **1979**, *18* (4), 684−695.
(34) Liu, X. J.; Zhang, W. R.; Park, T. J. Modelling coal gasification in an entrained flow gasifier. *Combust. Theory Modell.* **2001**, *5* (4), 595−608.